

Quantum Monte Carlo Investigation of Exchange and Correlation in Silicon

Randolph Q. Hood,¹ M. Y. Chou,¹ A. J. Williamson,² G. Rajagopal,² R. J. Needs,² and W. M. C. Foulkes³

¹*School of Physics, Georgia Institute of Technology, Atlanta, Georgia 30332-0430*

²*Cavendish Laboratory, Madingley Road, Cambridge CB3 0HE, United Kingdom*

³*The Blackett Laboratory, Imperial College, Prince Consort Road, London SW7 2BZ, United Kingdom*

(Received 9 September 1996)

Realistic many-body wave functions for diamond-structure silicon are constructed for different values of the Coulomb coupling constant. The coupling-constant-integrated pair correlation function, the exchange-correlation hole, and the exchange-correlation energy density are calculated and compared with those obtained from the local density and average density approximations. We draw conclusions about the reasons for the success of the local density approximation and suggest a method for testing the effectiveness of exchange-correlation functionals. [S0031-9007(97)02969-4]

PACS numbers: 71.15.Mb, 71.10.-w, 71.45.Gm

The standard computational tool of electronic-structure theory for solids is the local density approximation (LDA) within density-functional theory [1,2]. This has been applied successfully to systems, including those with quite rapidly varying densities, even though the LDA is based on approximating the system as locally homogeneous. However, when discrepancies between experiment and theory in solids arise it is difficult to improve upon the LDA systematically, although several schemes have been devised [3,4]. Since there is currently limited guidance for making improvements, we have used coupling constant integration and variational quantum Monte Carlo (VMC) techniques to calculate the quantities of central importance in density functional theory for a realistic inhomogeneous anisotropic solid. We have calculated the coupling-constant-integrated pair correlation function, the exchange-correlation hole, and the exchange-correlation energy density of diamond-structure silicon. In this Letter we describe our approach along with the insights gained by comparing these quantities with those from the LDA and the average density approximation (ADA) [3].

In Kohn-Sham density functional theory there is an exact relationship [5] between the exchange-correlation energy, E_{xc} , and the ground state many-electron wave functions Ψ_λ associated with the different values of the Coulomb-coupling constant, λ . The electronic density of each Ψ_λ must equal the density at full coupling ($\lambda = 1$). This condition can be ensured by adding an additional external potential $v_\lambda(\mathbf{r})$ to the many-body Hamiltonian in which the electron-electron interaction is multiplied by λ . The coupling-constant-integrated pair correlation function $\bar{g}(\mathbf{r}, \mathbf{r}')$, the exchange-correlation hole $\rho_{xc}(\mathbf{r}, \mathbf{r}')$, and the exchange-correlation energy density $e_{xc}(\mathbf{r})$ are related by [6]

$$e_{xc}(\mathbf{r}) = \frac{n(\mathbf{r})}{2} \int d\mathbf{r}' \frac{\rho_{xc}(\mathbf{r}, \mathbf{r}')}{|\mathbf{r} - \mathbf{r}'|}, \quad (1)$$

$$\rho_{xc}(\mathbf{r}, \mathbf{r}') = n(\mathbf{r}') [\bar{g}(\mathbf{r}, \mathbf{r}') - 1]. \quad (2)$$

The total exchange-correlation energy, E_{xc} , is obtained by integrating $e_{xc}(\mathbf{r})$ over all space. Writing \bar{g} in terms of its

constituent spin components

$$\bar{g}(\mathbf{r}, \mathbf{r}') = \sum_{\alpha, \beta} \frac{n_\alpha(\mathbf{r})n_\beta(\mathbf{r}')}{n(\mathbf{r})n(\mathbf{r}')} \bar{g}_{\alpha\beta}(\mathbf{r}, \mathbf{r}') \quad (3)$$

yields an equation involving the many-electron wave functions,

$$\bar{g}_{\alpha\beta}(\mathbf{r}, \mathbf{r}') = \frac{N(N-1)}{n_\alpha(\mathbf{r})n_\beta(\mathbf{r}')} \int_0^1 d\lambda \int d\mathbf{x}_3 \cdots d\mathbf{x}_N \times |\Psi_\lambda(\mathbf{r}\alpha, \mathbf{r}'\beta, \mathbf{x}_3, \dots, \mathbf{x}_N)|^2, \quad (4)$$

where N is the number of electrons, $n_\alpha(\mathbf{r})$ is the electronic density for spin α , and \mathbf{x}_i denotes the i th electron's spatial and spin components. In an unpolarized system such as silicon Eq. (3) reduces to $\bar{g} = \frac{1}{4} \sum_{\alpha, \beta} \bar{g}_{\alpha\beta}$. Together Eqs. (1)–(4) specify the exact relationship between $e_{xc}(\mathbf{r})$ and the many-body wave functions, and forms the basis of the calculations in this paper.

For our calculations we used a simulation cell consisting of $3 \times 3 \times 3$ primitive fcc unit cells of the diamond lattice, and containing 216 valence electrons. A norm-conserving nonlocal LDA pseudopotential was used to model the core electrons. The electron-electron interaction was modeled using the form described in Ref. [7], which virtually eliminates the finite size effect arising from the use of Coulomb interactions in periodic boundary conditions. Slater-Jastrow wave functions containing 22 free parameters were used for Ψ_λ , and the Jastrow factors were constrained to obey the λ -dependent cusp conditions. The single-particle orbitals in the Slater determinant were obtained from LDA calculations, and the values of the 22 parameters in the Jastrow factors were optimized by minimizing the variance of the energy [8]. A detailed description of this form of wave function can be found in Ref. [9]. Our VMC calculations follow the methodology described in Ref. [10]. Comparison with diffusion Monte Carlo results showed that our wave function for $\lambda = 1$ retrieves 85% of the fixed-node correlation energy.

As an initial approximation for v_λ we used

$$v_\lambda(\mathbf{r}) = (1 - \lambda) \int d\mathbf{r}' \frac{n(\mathbf{r}')}{|\mathbf{r} - \mathbf{r}'|} + v_{\text{xc},\lambda=1}^{\text{LDA}}(n(\mathbf{r})) - v_{\text{xc},\lambda}^{\text{LDA}}(n(\mathbf{r})),$$

which would ensure that the density was independent of λ in an LDA calculation. The value of $v_{\text{xc},\lambda}^{\text{LDA}}(n)$ was obtained from the exact scaling relation [11], $v_{\text{xc},\lambda}^{\text{LDA}}(n) = \lambda^2 v_{\text{xc},\lambda=1}^{\text{LDA}}(n/\lambda^3)$. This approximation yielded charge densities in close agreement with $n_{\lambda=1}(\mathbf{r})$. This approximation should be reliable for systems where the LDA provides an accurate prediction of the ground state density. This is the case in silicon, where the LDA charge density agrees closely with experiment [12] and is indistinguishable from the density we found with VMC. The small residual deviations from the LDA density [13] were reduced by iteratively modifying the v_λ potentials and lastly by making a very small adjustment to the one-body function in the Jastrow term of the wave functions, which caused no discernible change in the total energy. The root mean square deviation of the final n_λ from the LDA density was less than 0.58% for all values of λ .

To obtain the quantities in Eqs. (1)–(4) requires an accurate representation of $g_{\alpha\beta}^\lambda$ throughout *all* of the six-dimensional space $\mathbf{r} \times \mathbf{r}'$, in contrast to previous calculations which obtained $g_{\alpha\beta}^{\lambda=1}$ at only a few points [14]. We have found that an efficient way to calculate and store this information is to expand $g_{\alpha\beta}^\lambda$ as a product of symmetrized plane waves $\phi_m(\mathbf{r})$,

$$g_{\alpha\beta}^\lambda(\mathbf{r}, \mathbf{r}') = \sum_{m,n} g_{\alpha\beta,mn}^\lambda \phi_m(\mathbf{r}) \phi_n^*(\mathbf{r}').$$

The number of independent coefficients was considerably reduced by using the full space group symmetry of the crystal. A plane wave cutoff of 23 Ry was used, corresponding to 82 616 independent coefficients. No significant changes in $g_{\alpha\beta}^\lambda$ were observed when this cutoff was increased to 38 Ry. At each λ all of the coefficients were accumulated simultaneously with the Monte Carlo Metropolis method using approximately 5.8×10^6 statistically independent configurations. For $\lambda = 0$, $g_{\alpha\beta}^\lambda$ can be generated directly from the single-particle functions. By comparing the Monte Carlo sampled and directly calculated functions we estimated the statistical error in \bar{g} to be between 1% and 6%. The noise was largest where the electronic density takes its smallest value, and smallest where the electronic density was largest. We also used direct calculations to investigate the effects of the finite size of the simulation cell on $g_{\alpha\beta}^{\lambda=0}$, which were found to be unimportant.

The integral over λ in Eq. (4) was evaluated numerically using five values of λ : 0, $\frac{1}{4}$, $\frac{1}{2}$, $\frac{3}{4}$, and 1. With increasing λ the exchange-correlation energy, U_{xc}^λ , where $E_{\text{xc}} = \int_0^1 U_{\text{xc}}^\lambda d\lambda$, was found to decrease smoothly and monotonically as shown in Fig. 1, as has been predicted

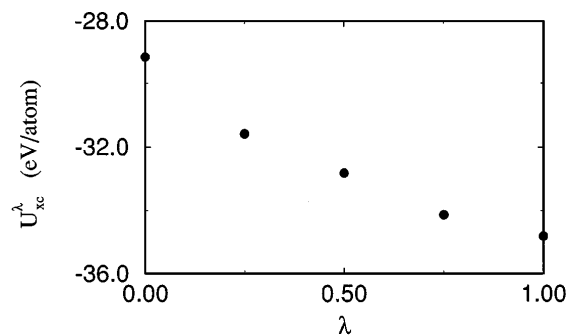


FIG. 1. The exchange-correlation energy, U_{xc}^λ , as a function of the coupling constant, λ . The statistical error bars are smaller than the symbols.

by Levy and Perdew [15]. As a further test, the identity

$$T^{\lambda=0} + E_{\text{xc}} = T^{\lambda=1} + U_{\text{xc}}^{\lambda=1}$$

was found to hold within 0.1%, where $T^{\lambda=1}$ is the fully interacting kinetic energy and $T^{\lambda=0}$ is the noninteracting kinetic energy appearing in density functional theory. Fewer than five values of λ was insufficient to satisfy this equation. Other quantities investigated such as the Jastrow term in the many-body wave function, and $g_{\alpha\beta}^\lambda$ displayed a smooth monotonic dependence on λ .

Figures 2(a), 2(b), and 2(c) show \bar{g} with electron position \mathbf{r} fixed on the bond center and \mathbf{r}' ranging over the (110) plane, for parallel and antiparallel spins in VMC, and the spin averaged form in the LDA [16], respectively. The largest features are confined mainly to the bonding region where the first electron is located. This agrees qualitatively with the result found previously by Fahy *et al.* [14] for carbon at $\lambda = 1$. Around all of the numerous points investigated: (1) the parallel-spin correlation function exhibited little dependence on λ , indicating that exchange is the dominant interaction between parallel-spin electrons in silicon, (2) the antiparallel-spin correlation function systematically deepened and enlarged with increasing λ ; a result solely due to correlation, and (3) the antiparallel-spin correlation function was more isotropic than the parallel-spin correlation function. The two more distant local minima away from the bond in Fig. 2(a) result from an exchange effect, which can be traced to a simultaneous dip in the single-particle density matrix, associated with the Slater determinant of the noninteracting $\lambda = 0$ system, and a decrease in the electronic density along the [111] direction.

The charge density which multiplies \bar{g} in Eq. (2) can have a profound effect on the shape of ρ_{xc} . Figures 3(a) and 3(b) show \bar{g} and ρ_{xc} around the tetrahedral interstitial site. The three local minima in Fig. 3(b) result from the increase in the electronic density away from the tetrahedral site. In the LDA ρ_{xc} is written in terms of

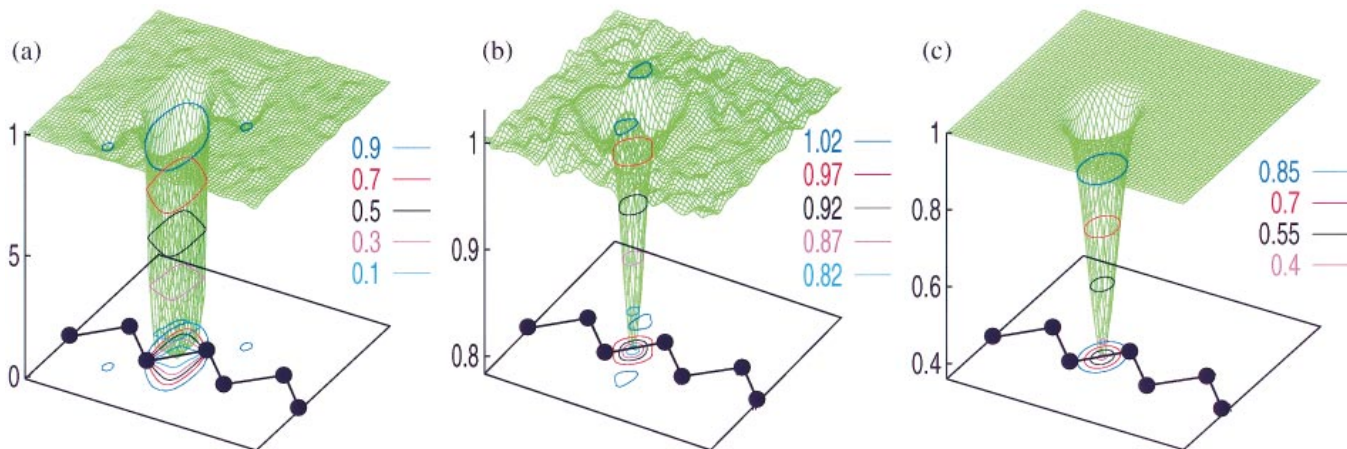


FIG. 2(color). The pair correlation function in the (110) plane for (a) parallel spin (VMC), (b) opposite spin (VMC), and (c) spin averaged (LDA), with one electron at the bond center. The atoms and bonds are schematically represented for bond chains along the [111] direction.

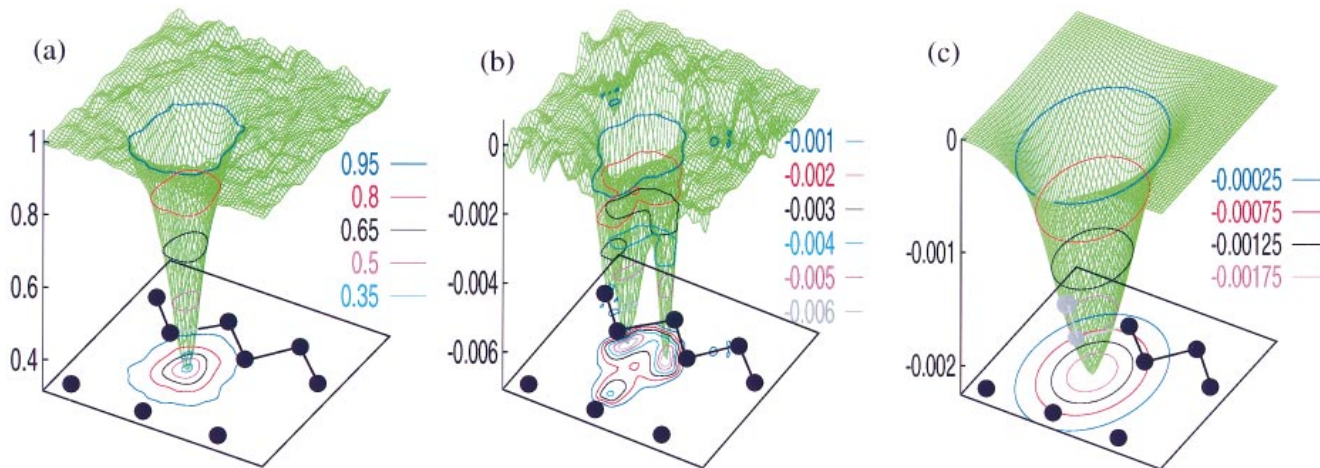


FIG. 3(color). The (a) spin-averaged pair correlation function (VMC), (b) exchange-correlation hole (VMC), and (c) exchange-correlation hole (LDA), with one electron fixed at the tetrahedral interstitial site in the (110) plane. The atoms and bonds are schematically represented for bond chains along the [111] direction.

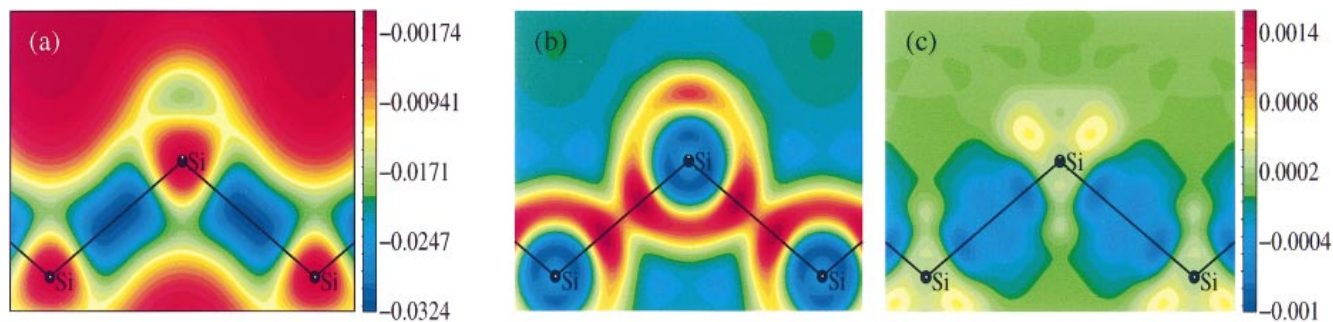


FIG. 4(color). Contour plots along the (110) plane for (a) $e_{xc}^{VMC}(\mathbf{r})$, (b) $e_{xc}^{VMC}(\mathbf{r}) - e_{xc}^{LDA}(\mathbf{r})$, and (c) $e_{xc}^{VMC}(\mathbf{r}) - e_{xc}^{ADA}(\mathbf{r})$. (b) and (c) have the same legend shown to the right of (c). The atoms and bonds are schematically represented for bond chains along the [111] direction.

\bar{g} of a homogeneous electron gas,

$$\rho_{xc}^{LDA}(\mathbf{r}, \mathbf{r}') = n(\mathbf{r}) \{ \bar{g}^{\text{hom}}(|\mathbf{r} - \mathbf{r}'|, n(\mathbf{r})) - 1 \}.$$

Note that the prefactor $n(\mathbf{r}')$ in Eq. (2) is replaced with $n(\mathbf{r})$ in the LDA to maintain the sum rule. This form results in an LDA hole with a localized shape as shown in Fig. 3(c) with a minimum value 3 times smaller than the VMC result. Around this interstitial point the LDA provides a better description of the shape of \bar{g} than of ρ_{xc} —the quantity that occurs in the exchange-correlation energy of Eq. (1). Note that only the spherical average of ρ_{xc} contributes to $e_{xc}(\mathbf{r})$ in Eq. (1).

Figure 4(a) shows the VMC exchange-correlation energy density, $e_{xc}^{\text{VMC}}(\mathbf{r})$, in the (110) plane calculated from Eqs. (1) and (2) using the sampled $\bar{g}(\mathbf{r}, \mathbf{r}')$. The difference from the LDA, $e_{xc}^{\text{VMC}}(\mathbf{r}) - e_{xc}^{\text{LDA}}(\mathbf{r})$, is shown in Fig. 4(b). The largest errors in the LDA occur in the bonding region where the electronic density is largest and around the pseudoatoms where it is smallest. The sharp features near the extrema of the electronic density in Fig. 4(b) result from the local nature of $e_{xc}^{\text{LDA}}(\mathbf{r})$. The true nonlocal functional includes information on the charge density in the neighboring region which tends to smooth out such sharp features. For this reason the nonlocal ADA yields a better overall agreement with our VMC result, as is shown in the difference, $e_{xc}^{\text{VMC}}(\mathbf{r}) - e_{xc}^{\text{ADA}}(\mathbf{r})$, in Fig. 4(c). The root mean square deviation of $e_{xc}(\mathbf{r})$ from $e_{xc}^{\text{VMC}}(\mathbf{r})$ was 4.9% for $e_{xc}(\mathbf{r}) = e_{xc}^{\text{LDA}}(\mathbf{r})$ and 2.0% for $e_{xc}(\mathbf{r}) = e_{xc}^{\text{ADA}}(\mathbf{r})$. The statistical error on the VMC evaluation of $e_{xc}^{\text{VMC}}(\mathbf{r})$ was estimated from a comparison of the exact $e_{xc}^{\lambda=0}(\mathbf{r})$ with the sampled form at $\lambda = 0$ to have a root mean square deviation of 0.5%, an order of magnitude smaller than the deviations observed between the LDA and VMC and 4 times smaller than the deviations between the ADA and VMC. (Note that the same nonlocal LDA pseudopotential was used in all three schemes.) Real-space plots of the exchange-correlation energy density are not provided here in the generalized gradient approximation, since this function typically contains an unphysical quantity that does not contribute to the total integrated energy in these approaches [17] (as in Perdew-Wang 91 [4]). The total integrated exchange-correlation energies E_{xc} (eV/atom) are -32.73 ± 0.01 (VMC), -32.75 (LDA), and -32.67 (ADA). The close agreement between the LDA and VMC exchange-correlation energies is due to a real-space cancellation of the bonding regions with the region around the pseudoatom and explains why the LDA does so well in describing silicon.

The coupling constant integration technique is a fruitful way to investigate the most relevant quantities in Kohn-Sham density functional theory. It is demonstrated in this Letter that this can be achieved by using realistic many-body wave functions generated with VMC. In silicon the principal effects of correlation are confined

mainly to antiparallel electrons as seen in $\bar{g}_{\alpha\beta}$. The spatial dependence of the electronic density that multiplies \bar{g} can have a profound influence on the shape of the exchange-correlation hole. The nonlocal nature of the functionals smooths the LDA exchange-correlation energy density. In addition to previously documented [3] subtle cancellations between the exchange and correlation, and the cancellations due to spherical averaging that occur in the LDA, there is also a real-space cancellation of errors in the exchange-correlation energy density in silicon. These and future calculations of exact exchange-correlation energy densities in real solids will make it possible to carry out stringent tests of the effectiveness of existing exchange-correlation functionals and should aid in the search for better functionals. The available data is no longer limited to a few numbers such as total energies, cohesive energies, and bulk moduli.

We thank M. Nekovee for helpful discussions. Financial support was provided under U.K. EPSRC Grants No. GR/K51198 and No. GR/K21061, EU Contract No. CHRX CT 94-0462, NSF Grant No. DMR-9157537, DOE Grant No. DE-FG05-90ER45431, and NATO Collaborative Research Grant No. CRG.951105. Our calculations are performed on the Cray-T3D at EPCC under EPSRC Grant No. GR/K42318, the Cray-T3D at PSC under Grant No. DMR-960004P, and the Hitachi SR2001.

-
- [1] P. Hohenberg and W. Kohn, Phys. Rev. **136**, B864 (1964).
 - [2] W. Kohn and L. J. Sham, Phys. Rev. **140**, A1133 (1965).
 - [3] O. Gunnarsson *et al.*, Phys. Rev. B **20**, 3136 (1979).
 - [4] J. P. Perdew, in *Electronic Structure of Solids '91*, edited by P. Ziesche and H. Eshrig (Akademie Verlag, Berlin, 1991); J. P. Perdew *et al.* (unpublished).
 - [5] For a derivation see, for example, R. M. Dreizler and E. K. Gross, *Density Functional Theory, An Approach to the Quantum Many-Body Problem* (Springer-Verlag, Berlin, 1990), pp. 183–185.
 - [6] We use Hartree atomic units ($\hbar = e = m = 4\pi\epsilon_0 = 1$) for all equations.
 - [7] A. J. Williamson *et al.*, Phys. Rev. B **55**, R4851 (1997); L. M. Fraser *et al.*, Phys. Rev. B **53**, 1814 (1996).
 - [8] C. J. Umrigar *et al.*, Phys. Rev. Lett. **60**, 1719 (1988).
 - [9] A. J. Williamson *et al.*, Phys. Rev. B **53**, 9640 (1996).
 - [10] S. Fahy *et al.*, Phys. Rev. B **42**, 3503 (1990).
 - [11] A. Görling and M. Levy, Phys. Rev. B **47**, 13 105 (1993).
 - [12] Z. W. Lu *et al.*, Phys. Rev. B **47**, 9385 (1993).
 - [13] In principle one should reduce the deviations in the density relative to $n_{\lambda=1}(\mathbf{r})$. However, we were unable to distinguish the small differences between $n_{\lambda=1}$ and n_{LDA} from the residual statistical noise.
 - [14] S. Fahy *et al.*, Phys. Rev. Lett. **65**, 1478 (1990).
 - [15] M. Levy and J. P. Perdew, Phys. Rev. A **32**, 2010 (1985).
 - [16] J. P. Perdew and Y. Wang, Phys. Rev. B **46**, 12947 (1992).
 - [17] J. P. Perdew (private communication).